Miniature Piezocone Penetration Test Results in Cohesive Soils

Daekyu Kim[1)], Mehmet T.Tumay[2)]

[1)] Assistant Professor, Department of Civil and Environmental Engineering, Sangmyung University, San 98-20, Anseo-Dong, Choen-An, South Korea, zip 330-720. daekyu@smu.ac.kr

[2)] Georgia Gulf Distinguished Professor Emeritus, Department of Civil and Environmental Engineering, College of Engineering, CEBA 3304 V, Louisiana State University, Baton Rouge, LA 70803.mtumay@eng.lsu.edu

ABSTRACT

The effects of penetration rate and filter element locations on the piezocone penetration and dissipation test results were experimentally studied. Ten piezocone tests were conducted utilizing U1 (filter element at the cone tip) and U2 (filter element above the cone base) miniature piezocone penetrometers. The calibration chamber tests were conducted on normally consolidated and heavily over-consolidated K33 specimens (mixture of 33 % kaolin and 67 % fine sand) under Ko conditions, and at penetration rates of 0.3, 0.6 and 2.0 cm/sec. The corrected net cone resistance and excess pore water pressure increased with the increase in penetration rate. The excess pore water pressure generated during penetration at U1 was larger than that generated at U2. The immediate (instantaneous) drop of excess pore water pressure at U1 and U2 locations, when penetration is arrested for pore pressure dissipation, was clearly identified by using a digital oscilloscope. The magnitude of the instantaneous drop in excess pore pressure affects the so-called "initial" pore pressures, and is influenced by pore pressure element location, speed of penetration and state of stress.

KEYWORDS: Calibration Chamber, Miniature Piezocone, Penetration Rate, Dissipation, Instantaneous Pore Pressure Drop.

1. INTRODUCTION

The piezocone penetration test (PCPT or CPTU) is widely used for the evaluation of *in-situ* soil properties and site characterization. The direct results from the piezocone penetration test are cone resistance, sleeve friction and pore water pressure. In addition, the data obtained from the change of excess pore water pressure (i.e. dissipation) following the arrest of intrusion are used in predicting soil compressibility and hydraulic conductivity. Thus many *in-situ* soil properties are obtained from the interpretation of the results of piezocone penetration and subsequent dissipation tests (Campanella and Robertson, 1981; Tumay and Acar, 1985; Kurup, 1993; Voyiadjis et al., 1994; Tumay et al., 1995). The interpretation of the piezocone test results is often complex as they are influenced by a number of variables related to the design of the cone, location of filter element, testing procedure, and soil characteristics (Tumay et al., 1982, 1998; Voyiadjis et al., 1994; Kurup et al., 1994a). The rate of penetration is one of the most important influencing factors related to the testing procedure. The cone resistance tends to decrease for penetration rates less than 2 cm/sec (standard rate of penetration) (Acar, 1981; Campanella and Robertson, 1981). The penetration rate has also an influence on excess pore water pressure and

Sleeve friction (Campanella and Robertson, 1981; Roy et al., 1982). Although previous studies, mostly

Received on 18/10/2006 and Accepted for Publication on 18/12/2007.

based on *in-situ* tests and conducted on sands, have revealed the penetration rate effect (Dayal and Allen, 1975; Vivatrat, 1978; Campanella et al., 1982; Almeida and Parry, 1985; Lunne et al., 1986; Konrad, 1987; Powell and Quarterman, 1988; Lunne et al., 1997), there still exists a need to further study the influence of penetration rate by using well-calibrated experimental equipment, under controlled testing schemes.

Calibration chamber tests are performed to calibrate *in-situ* testing devices. In a calibration chamber test, homogeneous, reproducible and instrumented soil specimens can be prepared with a known stress history, and various parametric studies can be performed under well-controlled boundary conditions. These features present a definite advantage of the calibration chamber test in the laboratory over alternative calibration by *in-situ* testing.

The effect of penetration rate, filter element location (U1 or U2) and interactions with over-consolidation ratio (OCR) on the results of piezocone test (i.e., cone resistance, pore water pressure, dissipation of excess pore water pressure and the instantaneous change of excess pore water pressure at the time of penetration arrest) have been investigated in this research. Systematic calibration chamber tests were conducted by using a specially fabricated miniature piezocone by Fugro B.V. The Netherlands, and the Louisiana State University Calibration Chamber System (LSU/CALCHAS).

The test results, experimental equipment and procedural details are presented in the following sections.

2. EXPERIMENTAL EQUIPMENT AND PROCEDURE

This section describes the experimental equipment and procedure of the miniature piezocone penetration and dissipation tests performed BY using the LSU/CALCHAS (Tumay and de Lima, 1992) and the slurry consolidometer (Kurup, 1993; Voyiadjis et al., 1993; Kurup et al., 1994a). Ten penetration tests were conducted using a special miniature piezocone with interchangeable filter element locations, at penetration rates of 0.3 cm/sec, 0.6 cm/sec and 2.0 cm/sec in normally consolidated (OCR=1) and heavily over-consolidated (OCR=10) specimens (Kim, 1999; Lim, 1999).

The procedure of the piezocone test is as follows. First, the dry soil sample was mixed with deaired and deionized water. The soil slurry was then placed in the slurry consolidometer for initial consolidation. After the initial consolidation, the soil specimen was transferred into the calibration chamber. The piezocone penetration and subsequent dissipation tests were conducted after reconsolidation in the calibration chamber.

Preparation of Soil Slurry and Slurry Consolidation

Soil slurry was prepared by mixing dry soil sample and deaired/deionized water at a water content of twice the liquid limit (circa 40%) by using a heavy duty chemical mixer. This water content was found to be appropriate to minimize air entrapment in the slurry during mixing and placement into the slurry consolidometer (Kurup, 1993; Kurup et al., 1994a). A mixture of 33% kaolin and 67% fine sand by dry weight was used to prepare the K33 soil specimen. The grain size distribution and Atterberg limits of the kaolin, the fine sand and the mixture are shown in Fig. 1.

Before pouring the soil slurry into the slurry consolidometer, a 1.59 mm thick rubber membrane was placed inside the slurry consolidometer to confine the specimen, and the pore pressure access ducts were instrumented to measure the pore water pressure at appropriate heights and radial locations (Fig. 2). The soil slurry was very carefully placed inside the slurry consolidometer minimizing entrapment of air bubbles. A 120-150 mm layer of pure sand was placed on top of the slurry separated by a sheet of filter paper. The sand layer provides effective upper drainage during slurry consolidation, and protects the top surface of the specimen from possible damage while transferring specimen from slurry consolidometer to calibration chamber for reconsolidation. The pore water pressure access ducts instrumented inside the slurry consolidometer were also deaired and kept saturated at all times.

The slurry consolidometer was designed and used to prepare large cohesive specimen by Kurup (1993) and Kurup et al. (1994a). The slurry consolidometer is composed of two PVC tubes. Each tube is 525 mm in inside diameter, 15 mm thick and 812 mm in height. The lower tube is split longitudinally into two halves that are held together by a metal frame to minimize disturbance of the soil specimen while transferring it into the calibration chamber. The upper tube serves as an additional storage compartment for the high water content slurry during the initial stage of consolidation. Seven pore water pressure access ducts, whose tips are located at various radial distances and at two different elevations, were instrumented inside the slurry consolidometer. The ducts were saturated by flushing with deaired water and assembled with the pressure transducer while submerged. The tips of the ducts were then immersed in deaired water and subjected to vacuum in the Nold DeAerator to ensure the saturation. They were connected to individual pressure transducers through the base plate (Fig. 3). The tip of the duct was sealed with porous plastic filter material to prevent the clogging of the tube. Fig. 4 shows the consolidation in the slurry consolidation, and Fig. 5 shows the schematic of the slurry consolidometer system.

A consolidation stress of 206.85 kPa was applied to the soil slurry. This vertical stress was selected under the consideration of the rigid boundary effect of the slurry consolidometer, and to obtain an initial soil specimen of sufficient strength for self-standing. The change of pore water pressure during the consolidation in the consolidometer was monitored from the access ducts and the data acquisition system. The loading system for slurry consolidation consists of a hydraulic cylinder jack powered by an air hydraulic pump and an aluminum piston plate with a steel piston rod and holes for drainage and backpressure. The pump has an automatic pressure make-up feature. The load from the push jack is transferred to the soil through the piston rod and the piston plate.

Reconsolidation in Calibration Chamber

After the consolidation in the slurry consolidometer, the upper tube of the consolidometer was removed and the top surface of the specimen (i.e. top sand layer) was trimmed at an appropriate height. Then the specimen was transferred into the calibration chamber using an overhead crane. The lower tube of the slurry consolidometer was removed carefully not to disturb the specimen, and the inner shell and the outer shell of the calibration chamber were placed through the specimen. After that, the reconsolidation of the specimen was performed using LSU/CALCHAS. The specimen was subjected to the effective vertical stress of 262.01 kPa, a higher consolidation stress than that in slurry consolidometer, under Ko condition. This technique is known to produce cohesive soil specimens of very high quality (Huang et al., 1988; Kurup et al., 1994a). The value of Ko was recorded as 0.42 for normally consolidated specimen (OCR=1), and 1.58 for heavily over-consolidated specimen (OCR=10) at the end of the reconsolidation. Fig. 6 and Fig. 7 show the LSU/ CALCHAS.

LSU/CALCHAS was designed by de Lima (1990) de Lima and Tumay (1991), and Tumay and de Lima (1992). It consists of a piston cell, a control panel, a backpressure system, data acquisition/control software and a flexible double wall chamber that makes Ko condition possible. The internal diameters of the inner and outer shells of the flexible double wall chamber were 560 mm and 580 mm, respectively. The two cylindrical shells were 6.35 mm thick and were made of stainless steel. Deaired water was filled between the specimen and the inner shell and between the inner shell and the outer shell. The lateral stress was applied to the specimen from the double wall chamber. The double could chamber can hold the specimen, and was 525 mm in diameter and 815 mm in height. The top lid made of aluminum has holes for penetration test in addition to the holes for drainage. These holes were sealed using adapters during reconsolidation. The backpressure system was added to LSU/CALCHAS to ensure the saturation of the specimen (Kurup 1993). The piston cell was also a double walled cylinder. The inner cell was kept free for instrumentation and the outer cell between the two shells and the grooves at the bottom of the piston plate were filled with deaired

water. The piston was raised to apply the vertical stress to the specimen by pressurizing the water in the piston cell.

The control panel controls the vertical and lateral stresses independently. The lateral double wall chamber and the piston cell can be pressurized using the pneumatic transducers by digital to analog signals sent from a personal computer through a data acquisition board. The control panel also has pressure regulators for manual control of the stresses. The change of pore water pressure can be monitored from the data acquisition system and the pore water pressure access ducts instrumented at the beginning of the experiment.

Using the equipment described above, LSU/CALCHAS can simulate the boundary conditions such as BC1: constant vertical stress and constant lateral stress, BC2: zero vertical strain and zero lateral strain, BC3: constant vertical stress and zero lateral strain, and BC4: zero vertical strain and constant lateral stress. All penetration tests in this investigation were conducted under BC3 boundary condition.

Miniature Piezocone Penetration Test

When the reconsolidated sample was ready for testing, the miniature piezocone was saturated, and penetration and subsequent dissipation tests were conducted by using the hydraulic and chucking system at the rates of 0.3 cm/sec, 0.6 cm/sec and 2.0 cm/sec. Cone tip resistance and pore water pressure during penetration test and the change of pore water pressure during dissipation test were measured by the data acquisition system. In addition to the normal data acquisition system, as a unique feature of this investigation, a high-speed digital oscilloscope was used to record the instantaneous and very rapid change of pore water pressure when the penetration is stopped (arrested) for dissipation test. The results of miniature piezocone penetration and dissipation tests are presented in the following section.

Table 1 shows the piezocone test program. Six piezocone penetration and dissipation tests were conducted on normally consolidated specimens, and four piezocone tests were performed on heavily over-consolidated specimens. Both consolidations for the normally consolidated state and for the heavily over-consolidated state were performed under Ko condition. The value of Ko was recorded to be 0.42 for normally consolidated specimen and 1.58 for heavily over-consolidated specimen at the end of reconsolidation phase in the calibration chamber.

Table (1): Piezocone Test Program.

Filter Location	σ_v' (kPa)	σ_h' (kPa)	Ko	OCR	Penetration Rate (cm/sec)	Test Identification
U1	262.01	110.04	0.42	1.0	0.3	0.3cm/sec(U1,NC)
U2	262.01	110.04	0.42	1.0	0.3	0.3cm/sec(U2,NC)
U1	262.01	110.04	0.42	1.0	0.6	0.6cm/sec(U1,NC)
U2	262.01	110.04	0.42	1.0	0.6	0.6cm/sec(U2,NC)
U1	26.20	41.40	1.58	10.0	0.6	0.6cm/sec(U1,OC)
U2	26.20	41.40	1.58	10.0	0.6	0.6cm/sec(U2,OC)
U1	262.20	104.80	0.40	1.0	2.0	2.0cm/sec(U1,NC) (Lim 1999)
U2	262.20	104.80	0.40	1.0	2.0	2.0cm/sec(U2,NC) (Lim 1999)
U1	24.20	40.71	1.68	10.8	2.0	2.0cm/sec(U1,OC) (Lim 1999)
U2	24.20	40.71	1.68	10.8	2.0	2.0cm/sec(U2,OC) (Lim 1999)

The miniature piezocone penetrometer specially fabricated by Fugro B.V., the Netherlands, was used for the tests. It has a projected cone area of 100 mm^2, a cone apex angle of 60°, a friction sleeve area of 1 526 mm^2 and a slope sensor. The maximum load capacity is 9 kN. The miniature piezocone penetrometer has two interchangeable alternatives for the filter location. The filter can be located at the cone tip (U1 configuration) or at 1 mm above the base of the cone (U2 configuration) (Kurup et al., 1994a). The saturation of the filter elements and the transducer cavity is a very important step to avoid a slow and sluggish pore water pressure response during the penetration and dissipation tests. Therefore, the multi-stage deairing technique was used in this research. The filter elements were first boiled in water and cleaned by using an ultra-sonic cleaner, then saturated by applying vacuum in the Nold DeAerator (Juran and Tumay, 1989). The transducer cavity was flushed with deaired water in a funnel of deaired water using a syringe. Then the saturated filter elements and the cone tip were assembled in the funnel of deaired water. Finally, the assembled piezocone was once again subjected to vacuum in the Nold DeAerator.

The hydraulic system was mounted on the calibration chamber for the penetration and extraction of the piezocone penetrometer in a single stroke of maximum 640 mm. It consists of a dual piston and a double acting hydraulic jack mounted on a collapsible frame. The push jack is equipped with a chucking system to grab the piezocone during penetration and extraction (Fig. 8).

All data during the test were recorded by using the data acquisition system as shown in Fig. 6. The penetration depth was measured by using the depth decoding system capable of registering penetration depth in millimeter range. As the cone advances, the disk turns mechanically and the electric analog signal is converted to a digital signal, and the depth is recorded by using the data acquisition software. As a special feature, a high-speed digital oscilloscope was used to measure the instantaneous rapid change (i.e. sampling rate in milliseconds) of pore water pressure when the penetration stopped for dissipation test. Details regarding mini-piezocone penetration test using LSU/CALCHAS are described in de Lima (1990), Kurup (1993), Kim (1999) and Lim (1999).

3. Test Results

In this section, the results of the penetration and dissipation tests (cone resistance, pore water pressure and the change of pore water pressure after penetration arrest) are presented. As shown in the piezocone test program (Table 1), 0.3 cm/sec (U1, NC) implies the test conducted by using U1 configuration piezocone (filter element at cone tip) and normally consolidated specimen (OCR=1) at penetration rate of 0.3 cm/sec. Similarly, 0.6 cm/sec (U2, OC) indicates the test conducted by using U2 configuration piezocone (filter element 1 mm above the cone base) and heavily over-consolidated specimen (OCR=10) at penetration rate of 0.6 cm/sec. All the tests in Table 1 are identified in the same manner.

Cone Resistance

The cone resistance was expressed as the corrected net cone resistance obtained by subtracting the chamber backpressure from the corrected cone resistance. A backpressure of 70 kPa was applied to ensure saturation (B=1) and compliance of pore pressure measurements. The corrected cone resistance was, as shown in Fig. 9, obtained from the measured cone resistance and the pore water pressure measured above the cone base (Campanella and Robertson, 1981; Tumay and Acar, 1985; Kurup, 1993). The area ratio of the miniature piezocone used in this research was 0.62. Fig. 10 to Fig. 12 present the corrected net cone resistance profiles. For all tests, a peak cone resistance, larger than the steady value, occurred at a depth of 10 cm (sand layer) before the steady state penetration was reached. The peak cone resistance occurs to initiate the penetrations and can be thought as the influence of the sand layer at the top of the specimen. The peak cone resistances were excluded to avoid complexity, and the steady values are presented in all figures.

The effect of penetration rate on the cone resistance is obvious as shown in Fig. 10 to Fig. 12. The steady value

of the corrected net cone resistance at higher penetration rate is greater than that at lower rate for all kinds of tests; that is, for U1 configuration piezocone and normally consolidated specimen as in Fig. 10, for U2 configuration piezocone and normally consolidated specimen as in Fig. 11 and for U1 and U2 configuration piezocones and heavily over-consolidated specimen as in Fig. 12. More specifically, the steady value of the cone resistance for normally consolidated specimen increased by 10 % both for U1 and U2 configurations with the increase in the penetration rate from 0.3 cm/sec to 0.6 cm/sec, and increased by 8 % with the penetration rate increase from 0.6 cm/sec to 2.0 cm/sec.

The steady values of the corrected net cone resistance, both for 0.3 cm/sec (U1, NC) and for 0.3 cm/sec (U2, NC), were 1.12 MPa, and the corresponding penetration depth values were 105 mm. The steady values of the corrected net cone resistances, both for 0.6 cm/sec (U1, NC) and for 0.6 cm/sec (U2, NC), were 1.23 MPa, and the corresponding penetration depth values were 130 mm. The steady values of the corrected net cone resistance both for 2.0 cm/sec (U1, NC) and for 2.0 cm/sec (U2, NC), were 1.34 MPa, and the corresponding penetration depth values were 190 mm. Accordingly, it can be said that the steady value of cone resistance and the corresponding depth are independent of the location of filter element, i.e., U1 or U2 configuration. For the heavily over-consolidated specimens (Fig. 12), comparing the cone resistance of 0.6 cm/sec (U1, OC) with that of 0.6 cm/sec (U2, OC), and the cone resistance of 2.0 cm/sec (U1, OC) with that of 2.0 cm/sec (U2, OC) also showed no discernable differences.

Comparing the cone resistance for normally consolidated specimen with that for heavily over-consolidated specimen shows that the cone resistance decreases with the decrease of the effective vertical stress. The corrected net cone resistance of 0.6 cm/sec (U1 and U2, NC) decreased by 12 % when the effective vertical stress decreased from 262.01 kPa to 26.20 kPa. The corrected net cone resistance of 2.0 cm/sec (U1 and U2, NC) decreased by 20 % when the effective vertical stress decreased from 262.20 kPa to 24.20 kPa.

Excess Pore Water Pressure

Fig. 13 to Fig. 15 show the excess pore water pressure profiles that were obtained by subtracting the chamber backpressure from the measured pore water pressure. The excess pore water pressure profiles to the depth of 10 cm (sand layer) were excluded, as in the cone resistance, to avoid complexity and the steady values are presented in all figures.

The steady values of excess pore water pressures for 0.3 cm/sec (U1, NC) 0.3 cm/sec (U2, NC), 0.6 cm/sec (U1, NC), 0.6 cm/sec (U2, NC), 2.0 cm/sec (U1, NC), and 2.0 cm/sec (U2, NC) were 0.067 MPa, 0.064 MPa, 0.086 MPa, 0.081 MPa, 0.535 MPa and 0.523 MPa, respectively. For heavily over-consolidated specimens, the steady values of excess pore water pressures for 0.6 cm/sec (U1, OC), 0.6 cm/sec (U2, OC), 2.0 cm/sec (U1, OC) and 2.0 cm/sec (U2, OC) were 0.063 MPa, 0.053 MPa, 0.308 MPa and 0.243 MPa, respectively. For all tests, it was clearly observed that the excess pore water pressures measured at the cone tip (U1 configuration) were invariably greater than those measured above the cone base (U2 configuration) at a specified penetration rate and for a specified over-consolidation ratio (OCR). This can be explained by the fact that the soil below the cone tip is subjected to predominantly normal stress. On the other hand, the soil above the cone base mainly experiences shear stress. Negative excess pore water pressures are often recorded just above the cone base for stiff over-consolidated clays (Tumay et al., 1982; Kurup, 1993; Kurup et al., 1994b). In this research, negative pore water pressures have not been measured even for the cases of OCR=10.

At a specified penetration rate, the excess pore water pressure under higher effective vertical stress was larger than that under lower effective vertical stress.

The excess pore water pressures associated with U1 configurations were higher than those of U2 configurations by 4.5 %, 6.2 % and 2.3 % for 0.3 cm/sec (NC), 0.6 cm/sec (NC) and 2.0 cm/sec (NC), respectively. For heavily over-consolidated specimens, the excess pore water pressures associated with U1 configurations were larger than those of U2

configurations by 19 % and 26 % for 0.6 cm/sec (OC) and 2.0 cm/sec (OC). There was no general relationship between the penetration rate and the magnitude of the difference of the excess pore water pressures of U1 configuration and U2 configuration; however, it might be deducted that the magnitude of the difference of the excess pore water pressures of U1 configuration and U2 configuration at a penetration rate is greater for over-consolidated specimen than for normally consolidated specimen.

Comparing the excess pore water pressures at various penetration rates indicated that excess pore water pressures measured both at the cone tip and above the cone base increase with the increase in penetration speed at a very similar rate.

Dissipation of Excess Pore Water Pressure

Fig. 16 to Fig. 18 present the dissipation curves of the excess pore water pressures, generated due to penetration, with respect to time. These unique experimental data were obtained with acquisition of pore pressure readings starting instantaneously when penetration was arrested. A millisecond data-sampling rate was used so as to capture "instantaneous" pore pressure variations. For general purposes, a data sampling rate in the order of seconds is normally used. The instantaneous initial excess pore water pressures normalized the excess pore water pressure data as in Fig. 16 to Fig. 18. Namely, the normalized excess pore water pressures were presented as the ratio of the measured pore pressures during dissipation to the instantaneous initial pore pressures measured at the filter element of the piezocone penetrometer immediately when the penetration stopped. This instantaneous pore pressure drop has not been previously considered in the literature. Generally, pore pressures are normalized by using so called "initial" pore pressures which are recorded within a time period of seconds.

The dissipations of excess pore water pressures in normally consolidated specimens generally took longer time than those in heavily over-consolidated specimens both for the U1 and U2 configurations. However, the greatest differences among all dissipation curves are the "instantaneous" initial values. Fig. 19 to Fig. 21 show the instantaneous initial segments of the dissipation data measured by using a high-speed digital oscilloscope. These instantaneous initial drops were higher for the pore water pressures measured at the cone tip (U1 configuration) than those measured above the cone base (U2 configuration). It is due to the redistribution of pore water pressure and to the sudden normal stress reduction that occur at the instant at which the penetration stops (Kurup, 1993; Kurup et al., 1994b; Voyiadjis et al., 1994; Tumay et al., 1995; Kurup and Tumay, 1997).

It was also found that the magnitude of the instantaneous initial drop for U1 configuration increased with the decrease in effective vertical stress (also expressed as OCR, see Table 1), and the excess pore water pressure nominally increased immediately after the initial drop for the case of 0.6 cm/sec (U2, OC) and 2.0 cm/sec (U2, OC). There seems to be no obvious effect of penetration rate on the magnitude of the instantaneous initial drop for the U2 configuration.

Grain Size Distribution after Piezocone Penetration

Fig. 22 shows the grain size distributions of the samples obtained after the penetration test. The samples were carefully extracted at certain radial distances away from the path of the piezocone penetration. Sieve analyses and hydrometer tests were performed for the samples. Sample 1, sample 2, sample 3 and sample 4 were obtained at radial distances between d (diameter of piezocone penetrometer) and 3d, between 3d and 5d, between 5d and 7d and between 7d and 9d, respectively, around the penetration hole. Fig. 22 depicts the granulometry of the sand, kaolin, original mixture used for the piezocone penetration tests (33 % kaolin and 67 % fine sand) and the samples 1 to 4.

It was observed that sample 3 and sample 4 (farthest from the penetration path) had almost the same grain size distributions as the original mixture, but sample 1 and sample 2 were clearly on the coarser side of the original mixture. This indicates that sample 1 and sample 2 contained less clay particles than the original mixture. Also, sample 1 (within a radial distance of 1 to cone

diameters) had less clay particles than sample 2.

It may be concluded, therefore, that the closer to the piezocone penetration path the sample is, the less clay fraction particles it contains. This can be explained by the fact that the clay fraction particles migrate radially from the axis of the penetration path. The clay fraction particles are carried in suspension by the water under pressure generated in soil pores by penetrometer intrusion. It maybe postulated that the migration would be more severe for faster rates of penetration, distorting the pore pressure dependent parameters, especially in soils with high D60/D10.

The change of the grain size distribution during the penetration test may affect the results and interpretation of the piezocone penetration test, i.e., cone resistance, excess pore water pressure, sleeve friction, and especially the results of dissipation tests. However, this effect of the change of grain size distribution has not yet been considered, and needs to be studied in future research.

4. Conclusions

In this research, the influences of penetration rate, filter element location and OCR (effective vertical stress in this research) on cone resistance, excess pore water pressure and dissipation of excess pore water pressure measured during dissipation tests were investigated. Ten miniature piezocone penetration and dissipation tests were conducted in a computer-controlled calibration chamber LSU/CALCHAS. Analysis of the test results with the previous experimental data led to the following conclusions:

1. Corrected net cone resistance increased with the increase in penetration rate.
2. The excess pore water pressure measured at the cone tip (U1 configuration) was greater than that measured above the cone base (U2 configuration).
3. The difference of the excess pore water pressures of U1 configuration and U2 configuration at a specified penetration rate was greater for over-consolidated specimen than for normally consolidated specimen.
4. The excess pore water pressures measured both at the cone tip and above the cone base increased with the increase in penetration speed at a very similar rate.
5. The excess pore water pressures at the cone tip and above the cone base were quite different. Furthermore, the excess pore water pressure at the cone tip changed very rapidly for all cases, which produced a large pore pressure gradient. In that sense, the importance of location of the filter element for measuring pore water pressure needs to be emphasized again.
6. The dissipation of excess pore water pressure for normally consolidated specimens took longer time than that for heavily over-consolidated specimens both for U1 and U2 configurations.
7. An instantaneous initial drop in excess pore water pressure, “immediately” after penetration arrest, was observed in all cases. The instantaneous initial drop in excess pore water pressure was higher for U1 configuration than for U2 configuration. The influence of the instantaneous pore pressure drop on the conventional “initial” pore pressures used in dissipation investigations needs further research.
8. Investigating the grain size distribution of samples along the path of penetration and dissipation tests, it has been observed that the soil, which was radially closer to the piezocone penetrometer, contained less clay particles than the soil which was farther from the piezocone penetrometer. This can be explained by the migration of clay particles in a radial direction mobilized by the water pressure generated in soil pores. The effect of this granulometry change on test results and interpretation needs further investigation.

Acknowledgments

The financial support for the work described in this paper was provided through an NSF grant CMS-9531782. Fugro, B.V., The Netherlands is acknowledged for their support of the project by fabricating the special mini

piezocone. Mr. Van Auker of Feldspar Corporation, Edgar, Florida donated the standard soils used in the project. Helpful suggestions by Professor Pradeep U. Kurup of University of Massachusetts, Lowell, MA and assistance in the conduct of the calibration tests by Dr. Beyongseock Lim, Messieurs William Tierney are gratefully acknowledged.

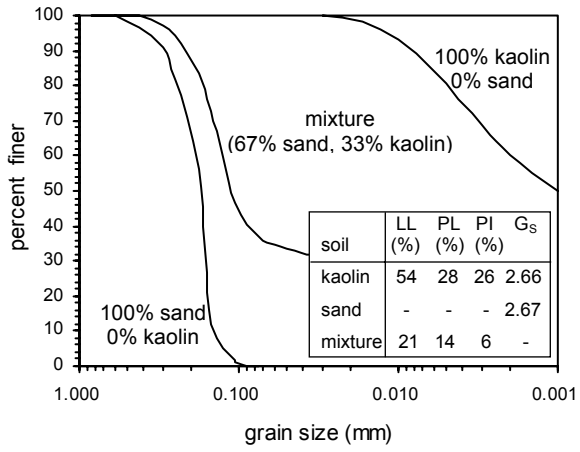

Fig. 1: Physical Properties of Soil Specimen (Kurup 1993).

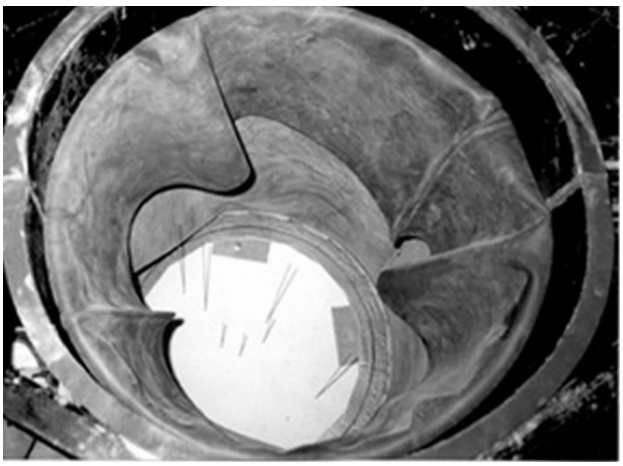

Fig. 2: Slurry Consolidometer with Membrane and Pore Water Pressure Access Ducts.

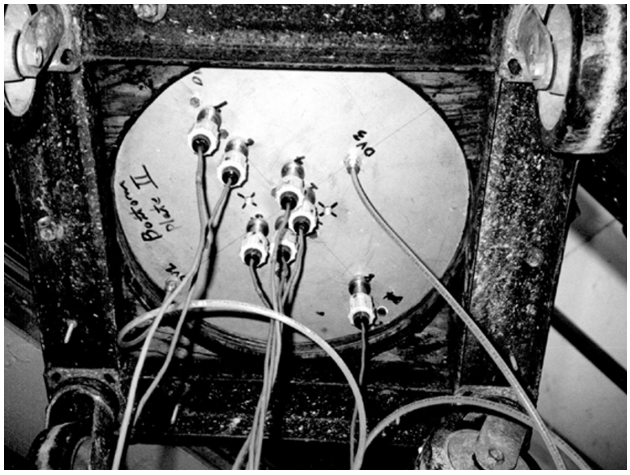

Fig. 3: Bottom of Base Plate with Pore Water Pressure Transducers.

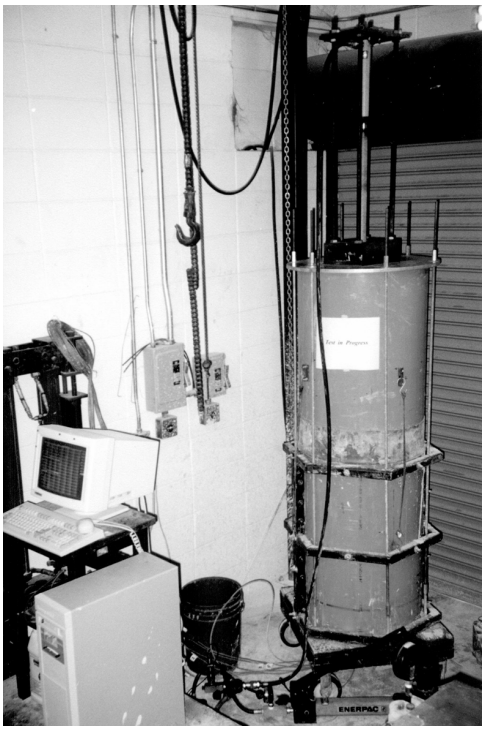

Fig. 4: Consolidation in Slurry Consolidometer.

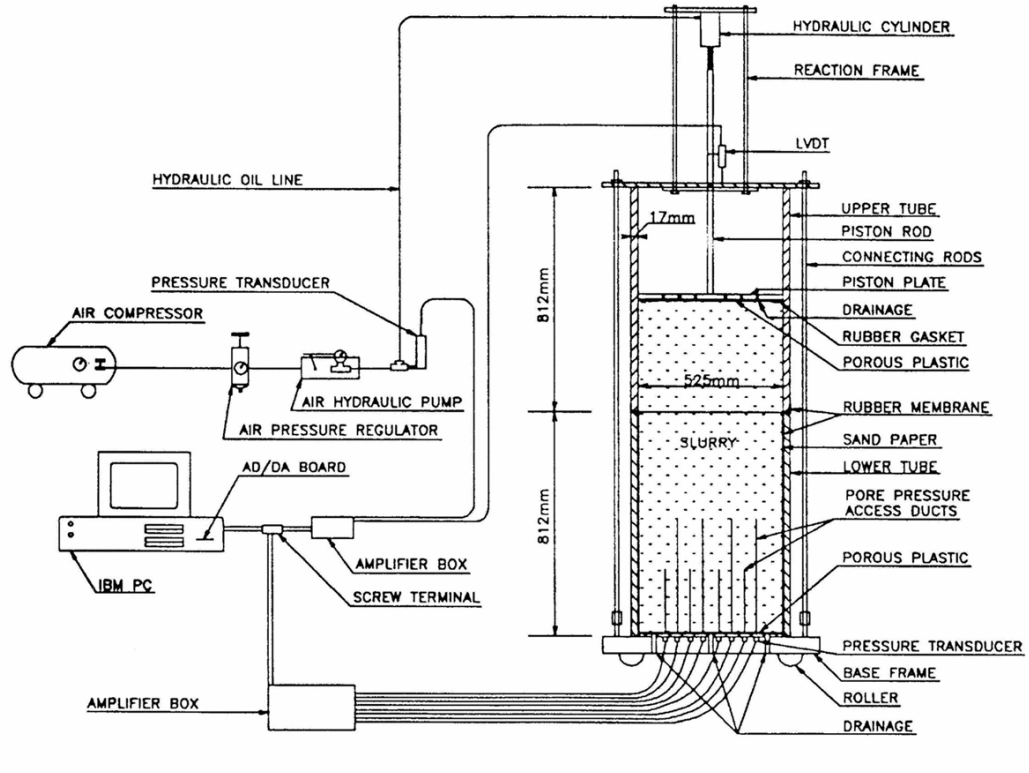

Fig 5: Schematic of Slurry Consolidometer System (Kurup, 1993).

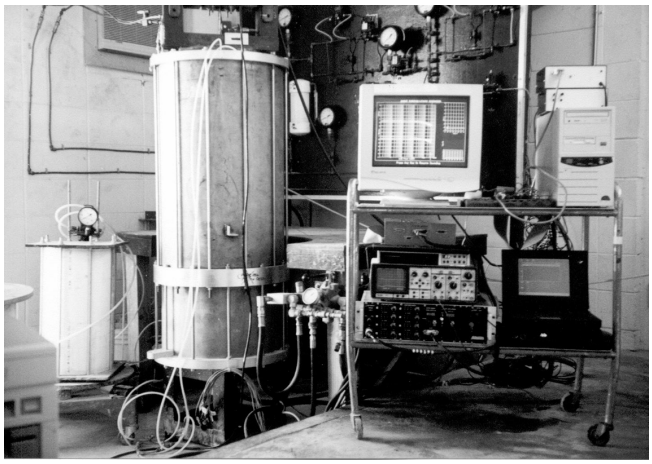

Fig 6: LSU/CALCHAS.

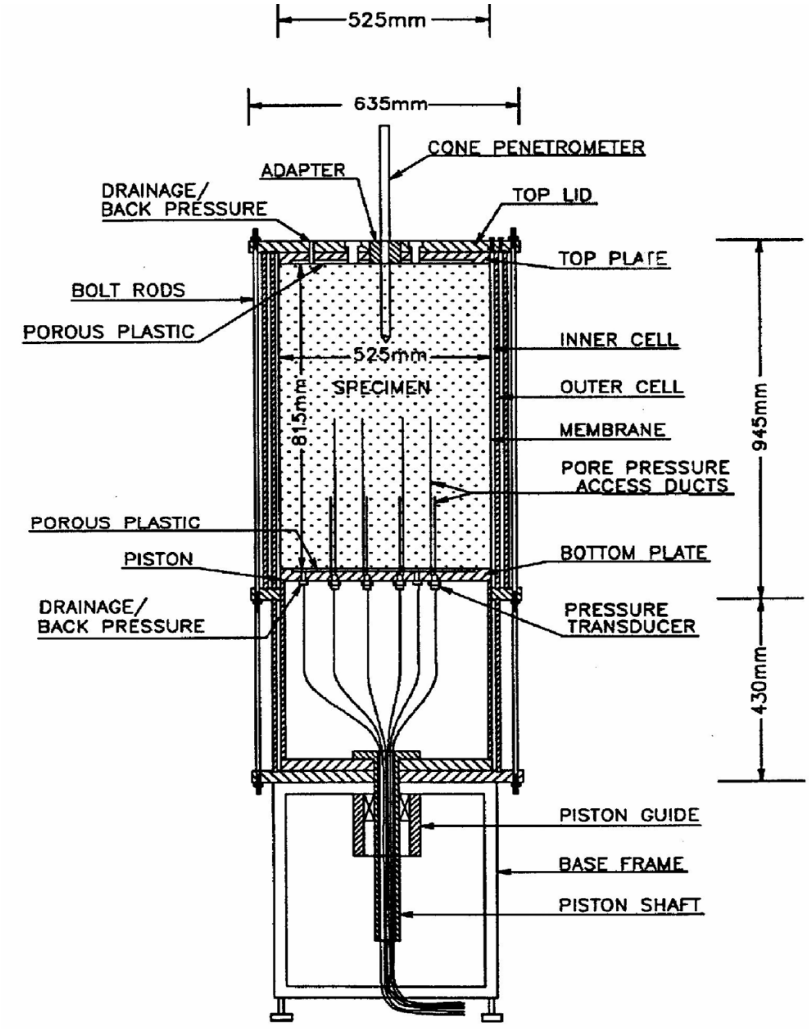

Fig 7: Schematic of Calibration Chamber (Kurup, 1993)..

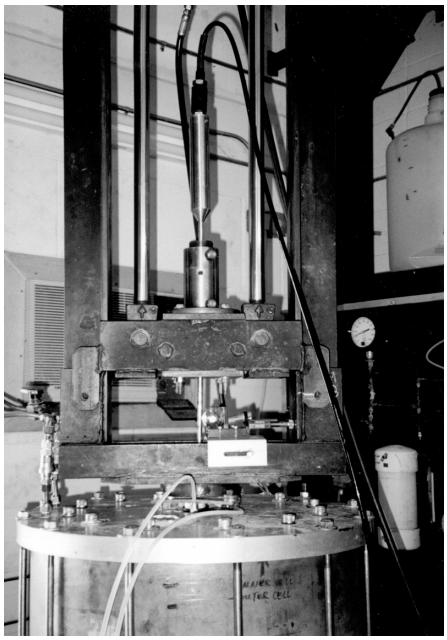

Fig 8: Piezocone Test By Using Hydraulic Jack.

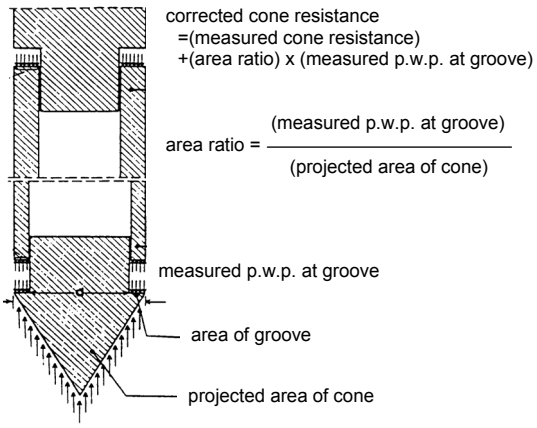

Fig. 9: Correction of Cone Resistance for Unequal End Area Effect.

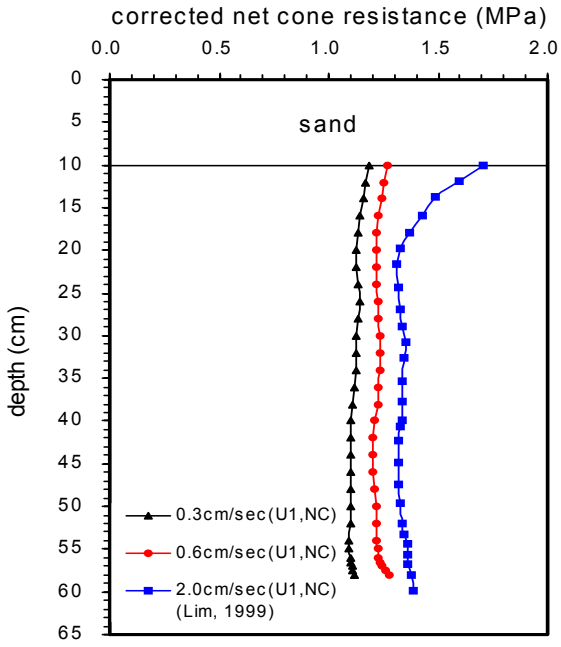

Fig. 10: Cone Resistance Profiles for U1 and NC Specimens.

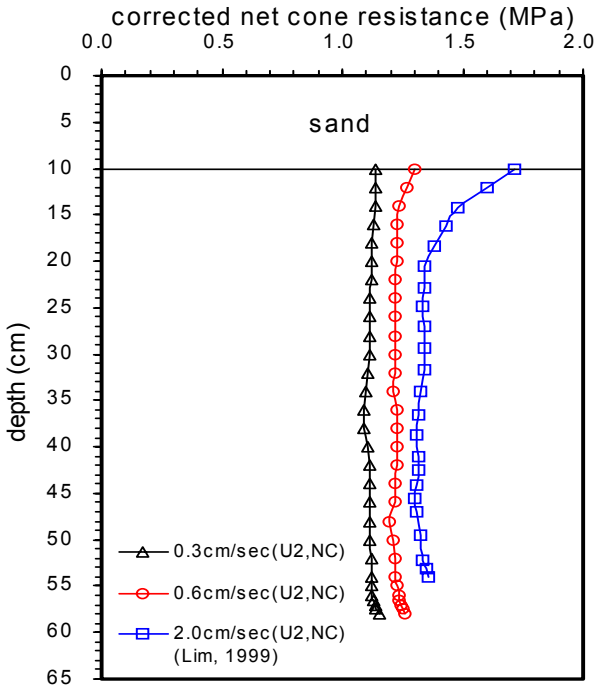

Fig.11: Cone Resistance Profiles for U2 and NC Specimens.

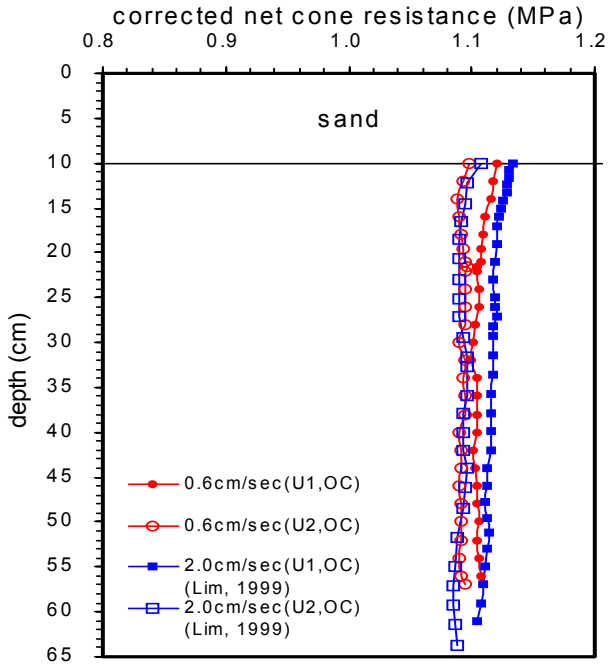

Fig.12: Cone Resistance Profiles for U1, U2 and OC Specimens.

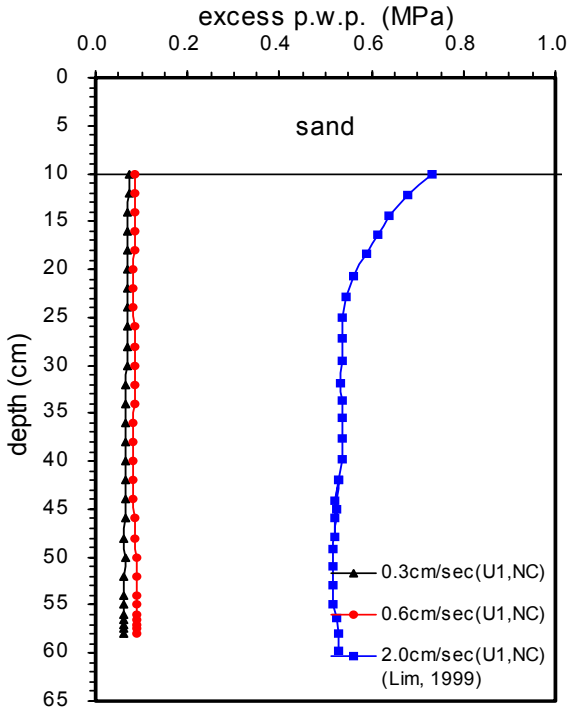

Fig. 13: Excess p.w.p. Profiles for U1 and NC Specimens.

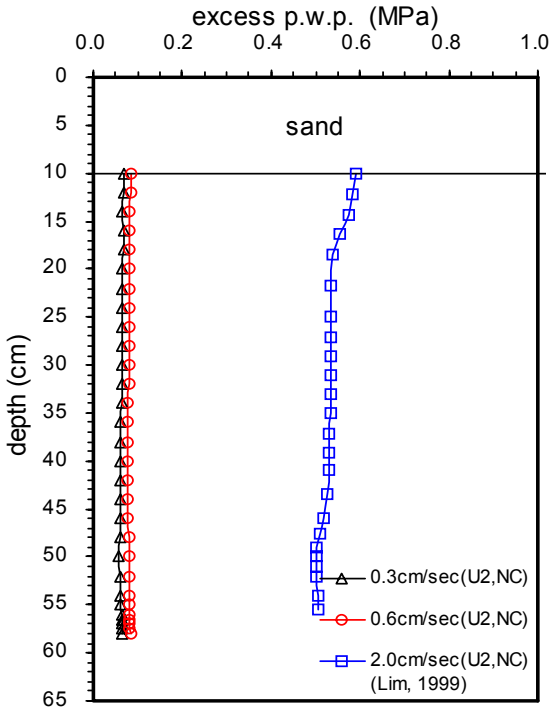

Fig. 14: Excess p.w.p. Profiles for U2 and NC Specimens.

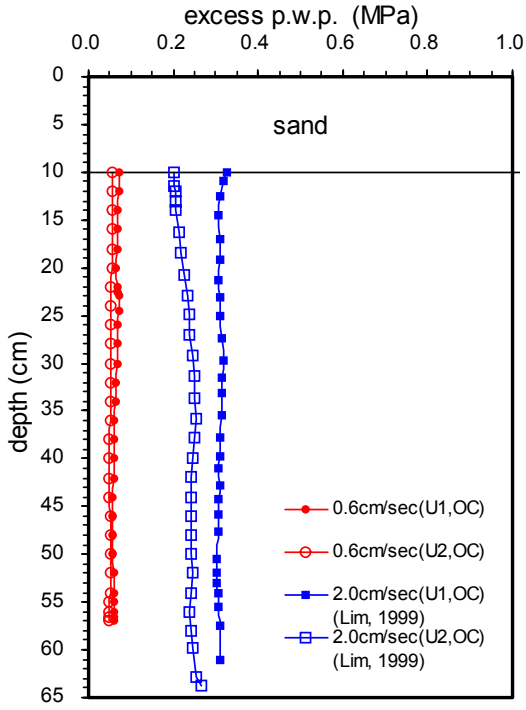

Fig. 15: Excess p.w.p. Profiles for U1, U2 and OC Specimens.

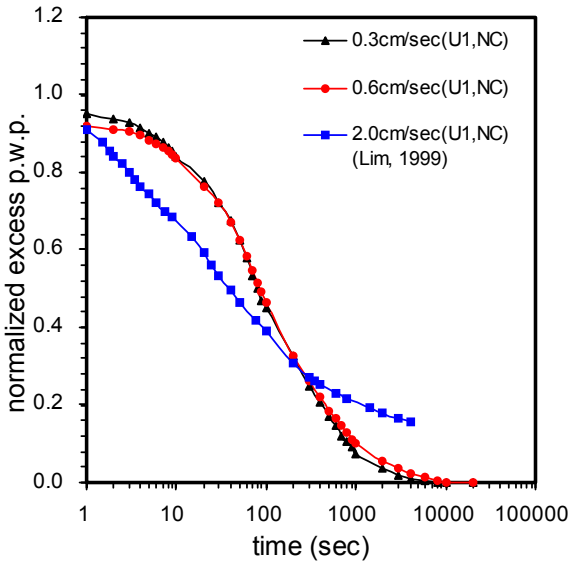

Fig. 16: Dissipation Curves for U1 and NC Specimens.

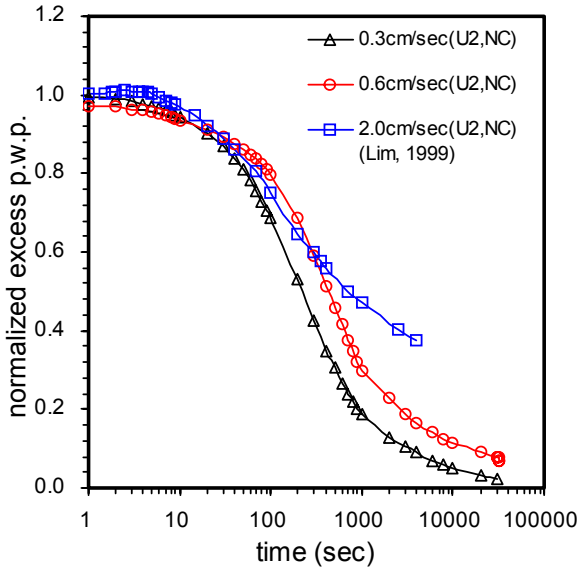

Fig. 17: Dissipation Curves for U2 and NC Specimens.

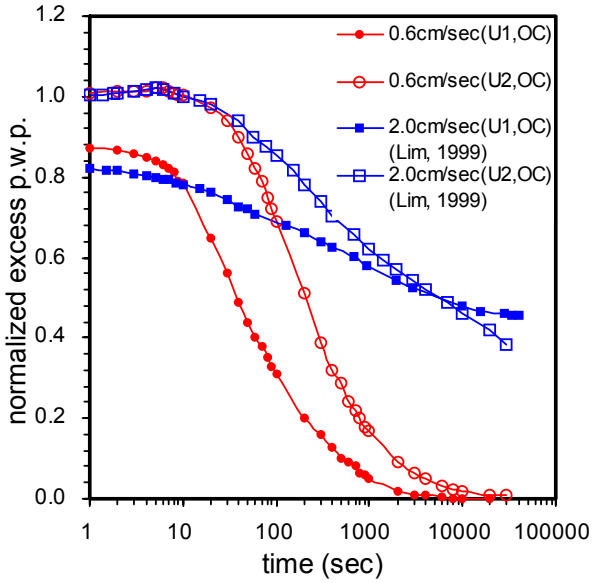

Fig. 18: Dissipation Curves for U1, U2 and OC Specimens.

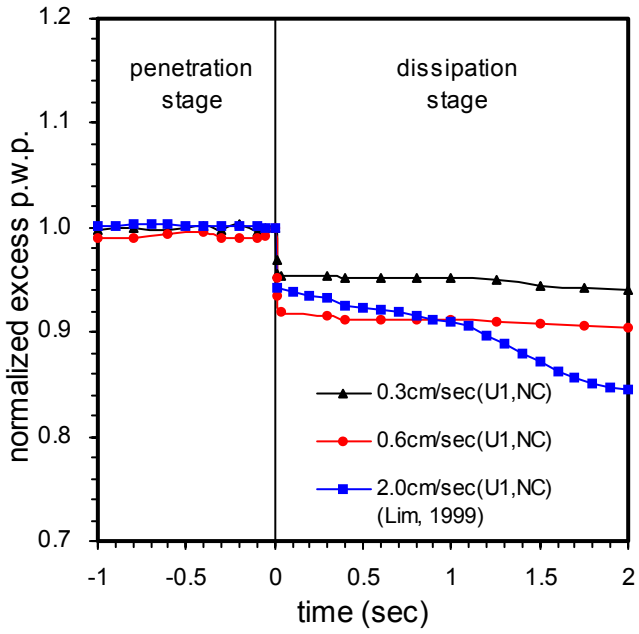

Fig. 19: Initial Parts of Dissipation Curves for U1 and NC Specimens.

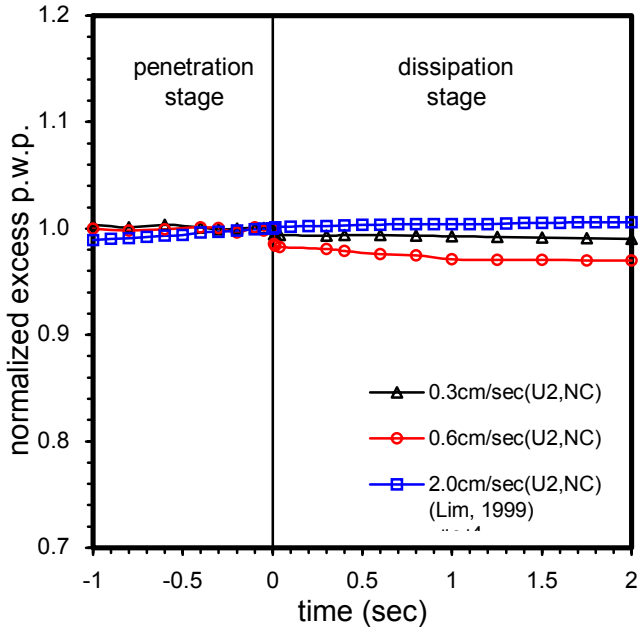

Fig. 20: Initial Parts of Dissipation Curves for U2 and NC Specimens.

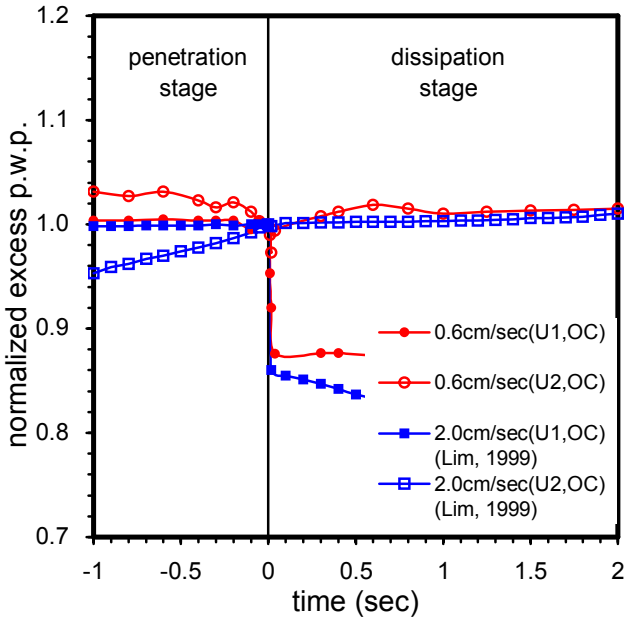

Fig. 21: Initial Parts of Dissipation Curves for U1, U2 and OC Specimens.

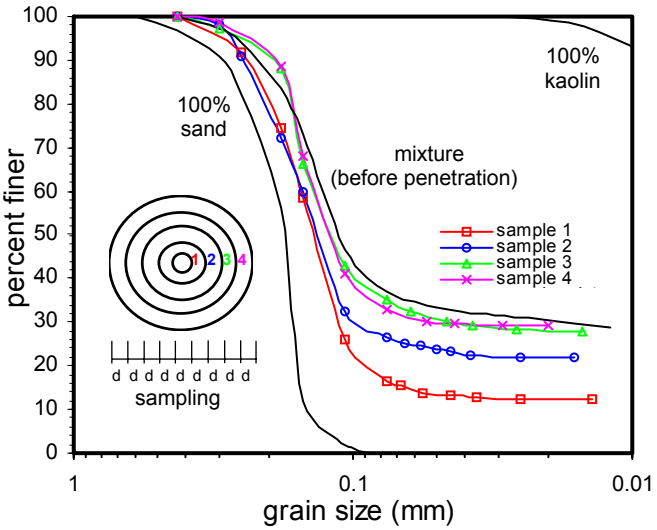

Fig. 22: Grain Size Distribution before and after Penetration Test.

REFERENCES

Acar, Y. B. (1981). *Piezocone penetration testing in soft cohesive soils*, Fugro Postdoctoral Geotechnical Engineering Report No. Ge-81/01, Louisiana State University, Baton Rouge, LA.

Almeida, M. S. S. and Parry, R. H. G. (1988). "Small Cone Penetrometer Tests in Laboratory Consolidated Clays." *Proceedings of the Int. Conf. on Penetration Testing, ISOPT-1*, Orlando, 2, Balkema Pub., Rotterdam, PP. 607-613.

Calmpanella, R. G., Gillespie, D. and Robertson, P. K. (1982). "Pore Pressure During Cone Penetration Testing." *Proceedings of the 2nd European Symposium on Penetration Testing, ESOPT-II,* Amsterdam, Balkema Pub., Rotterdam, PP. 507-512.

Campanella, R. G. and Robertson, P. K. (1981). "Applied Cone Research in Cone Penetration Testing and Experience." *R. M. Norris and R. D. Holtz (eds.), ASCE,* New York, NY, PP. 343-362.

Dayal, U. and Allen, J. G. (1975). "The effect of Penetration Rate on the Strength of Remoulded Clay and Sand Samples." *Canadian Geotechnical Journal,* 12(3), PP. 336-348.

De Lima, D. C. (1990). *Development, Fabrication and Verification of the LSU In-Situ Testing Calibration Chamber*, Ph.D. Dissertation, Louisiana State University, Baton Rouge, LA.

De Lima, D.C. and Tumay, M. T. (1991). "Scale Effects in Cone Penetration Tests." *ASCE, Geotechnical Engineering Congress 1991*, Boulder, CO., PP. 38-51.

Huang, A. B., Holtz, R. D. and Chameau, J. L. (1988). "Calibration Chamber for Cohesive Soils." *Geotechnical Testing Journal*, 11(1): 30-35.

Juran, I. and Tumay, M.T. (1989). "Soil Stratification Using the Dual Pore-Pressure Piezocone Test." *Transportation Research Record*, (1235), PP. 68-78.

Kim, D.K. (1999). *Numerical Simulation and Experimental Verification of Cone Penetration Rate And Anisotropy in Cohesive Soils*, Ph.D. Dissertation, Dept. of Civil and Environmental Engineering, Louisiana State University, Baton Rouge, LA.

Konrad, J. M. (1987). "Piezo-Friction-cone Penetrometer Testing in Soft Clays." *Canadian Geotechnical Journal,* 24, PP. 645-652.

Kurup, P. U. (1993). *Calibration Chamber Studies of Miniature Piezocone Penetration Tests in Cohesive Soil Specimens,* Ph. D. Dissertation, Department of

Civil and Environmental Engineering, Louisiana State University, Baton Rouge, LA.

Kurup, P. U. and Tumay, M. T. (1997). "A Numerical Model for the Analysis of Piezocone Dissipation Curves." *Proceedings of Int. Symposium on Numerical Models in Geomechanics (NVMOG VI),* Montreal, Canada, July 2-4, PP. 353-358.

Kurup, P. U., Voyiadjis, G. Z. and Tumay, M. T. (1994a). "Calibration Chamber Studies of Piezocone Test in Cohesive Soils." *Journal of Geotechnical Engineering,* 120(1): 81-107.

Kurup, P. U., Voyiadjis, G. Z. and Tumay, M. T. (1994b). "Excess Pore Pressure Dissipation after Piezocone Penetration." *Computer Methods and Advances in Geomechanics*, Siriwardane and Zaman (eds.), PP. 1751-1756.

Lim, B.S. (1999). *Determination of Consolidation Characteristics in Fine Grained Soils Evaluated by Piezocone Tests*. Ph.D. Dissertation, Department of Civil and Environmental Engineering, Louisiana State University, Baton Rouge, LA.

Lunne, T., Eidsmoen, T., Gillespie, D. and Howland, J. D. (1896). "Laboratory and Field Evaluation of cone penetrometers." *Proceedings of the ASCE Specialty Conf. In Situ '86: Use of in Situ Tests in Geotechnical Engineering*, Blacksburg, pp. 714-729.

Lunne, T., Robertson, P. K. and Powell J. J. M. (1997). *Cone Penetration Testing*. Blackie Academic and Professional, London.

Powell, J. J. M. and Quarterman, R. S. T. (1988). "The Interpretation of Cone Penetration Tests in Clays, with Particular Reference to Rate Effects." *Proceedings of the Int. Symposium on Penetration Testing, ISPT-I,* Orlando, 2, Balkema Pub., Rotterdam, PP. 903-910.

Roy, M., Tremblay, M., Tavenas, F. and La Rochelle, P. (1982). "Development of Pore Pressures in Quasi-static Penetration Tests in Sensitive Clay." *Canadian Geotechnical Journal,* 19, PP. 124-138.

Tumay, M. T. and Acar, Y. B. (1985). *Piezocone Penetration Testing in Soft Cohesive Soils.* ASTM, *STP 883*, R. C. Chaney and K. R. Demars (eds.), PP. 72-82.

Tumay, M. T., Acar, Y., Deseze, E. and Yilmaz, R. (1982). "Soil Exploration in Soft Clays with the Quasi-Static Electric Cone Penetrometer." *Proceedings of the 2nd European Symposium on Penetration Testing*, Amsterdam, PP. 915-921.

Tumay, M. T. and de Lima, D. C. (1992). *Calibration and Implementation of Miniature Electric Cone Penetrometer and Development, Fabrication and Verification of the LSU in Situ Testing Calibration Chamber (LSU/CALCHAS),* Department of Civil Engineering, Louisiana State University, Report (GE-92/08).

Tumay, M. T., Kurup, P. U. and Boggess, R. L. (1998). "A Continuous Intrusion of Electronic Miniature Cone Penetration Test System for Site Characterization." *Proceedings of 1st Int. Conf. on Site Characterization -ISC'98*, Atlanta, PP. 1183-1188.

Tumay, M. T., Kurup, P. U. and Voyiadjis, G. Z. (1995). "Profiling OCR and Ko from Piezocone Penetration Tests." *Proceedings, In. Symposium on Cone Penetration Testing*, Sweden, PP. 337-342.

Vivatrat, V. (1978). *Cone Penetration In Clays*, Ph. D. Thesis, Massachusetts Institute of Technology, Cambridge, Mass.

Voyiadjis, G. Z., Kurup, P. U. and Tumay, M. T. (1993). "Preparation of Large-size Cohesive Specimens for Calibration Chamber Testing." *Geotechnical Testing Journal*, GTJODJ, 16, (3): 339-349.

Voyiadjis, G. Z., Kurup, P. U. and Tumay, M. T. (1994). "Determination of Soil Properties from Laboratory Piezocone Penetration Tests." *13th Int. Conf. of Soil Mechanics and Foundation Engineering (XIII ICSMFE)*, India, PP. 303-308.

Voyiadjis, G. Z., Tumay, M. T. and Kurup, P. U. (1991). "Miniature Piezocone Penetration Tests on Soft Soils in a Calibration Chamber System." *Proceedings of Calibration Chamber Testing*, *of ISOCCT 1,* A. B. Huang (eds.), Elsevier Publishers, New York